The work was supported by Consejo de Desarrollo Cientifico y Tecnologico (CDCHT) (C-280) and Consejo Nacional de Investigaciones Cientificas y Tecnologicas (CONICIT).

References

[1] S. Wagner and P. M. Bridenbaugh, J. Crystal Growth **39**, 151 (1977).
[2] E. Parthe, Crystallochemie des structures tetraédriques, Gordon and Breach, Paris 1972 (p. 133).
[3] G. L. Hansen, J. L. Schmidt, and T. N. Casselman, J. appl. Phys. **53**, 7099 (1982).
[4] J. L. Shay and J. H. Wernick, Ternary Chalcopyrite Semiconductors: Growth, Electronic Properties, and Applications, Pergamon Press, Oxford 1975.
[5] A. Miller, A. MacKinnon, and D. Weaire, Solid State Phys. **36**, 119 (1989).
[6] V. P. Chernyavskii, N. A. Goryunova, and A. S. Borshchevskii, in: Chemical Bonds in Solids, Vol. 4, Ed. N. N. Sirota, Consultants Bureau, New York 1976 (p. 66).
[7] M. Quintero, L. Dierker, and J. C. Woolley, J. Solid State Chem. **63**, 110 (1986).
[8] J. C. Woolley and E. W. Williams, J. Electrochem. Soc. **113**, 899 (1966).
[9] L. Garbato and F. Ledda, J. Solid State Chem. **30**, 189 (1979).
[10] L. Garbato, F. Ledda, and P. Manca, Japan. J. appl. Phys. **19**, 67 (1980).
[11] M. Quintero, E. Guerrero, P. Grima, and J. C. Woolley, J. Electrochem. Soc., in the press.
[12] R. Chen and Y. Kirsh, Analysis of Thermally Stimulated Processes, Internat. Ser. Sci., Solid State, Vol. 15, Pergamon Press, 1981 (p. 97).
[13] R. G. Goodchild, O. H. Hughes, S. A. Lopez-Rivera, and J. C. Woolley, Canad. J. Phys. **60**, 1096 (1982).
[14] R. W. Chiang, D. F. O'Kane, and D. R. Mason, J. Electrochem. Soc. **113**, 849 (1966).
[15] L. Palatnik and E. I. Rogacheva, Soviet Phys. — Doklady **12**, 503 (1967).
[16] M. Quintero, P. Grima, R. Tovar, G. S. Pérez, and J. C. Woolley, phys. stat. sol. (a) **107**, 205 (1988).
[17] E. Guerrero, M. Quintero, and J. C. Woolley, J. Crystal Growth **92**, 150 (1988).
[18] L. Garbato, F. Ledda, P. Manca, A. Rucci, and A. Spiga, Progr. Crystal Growth Charact. **10**, 199 (1985).
[19] J. N. Gan, J. Tauc, V. G. Lambrecht, Jr., and M. Robbins, Phys. Rev. B **12**, 5797 (1975).
[20] E. Guerrero, M. Quintero, and J. C. Woolley, J. appl. Phys. **63**, 2252 (1988).
[21] J. A. van Vechten and T. K. Bergstresser, Phys. Rev. B **1**, 3351 (1970).
[22] J. E. Jaffe and A. Zunger, Phys. Rev. B **29**, 1882 (1984).
[23] K. Yoodee, J. C. Woolley, and V. Sa'yakanit, Phys. Rev. B **30**, 5904 (1984).

(Received June 2, 1988; in revised form October 17, 1988)

2. Experimental Methods

The alloys used were produced by the usual melt and anneal technique. The components of each 1.5 g sample were sealed under vacuum in a quartz capsule and melted together at 1150 °C. As in all such multi-component alloys, a suitable temperature of anneal is not easily determined until the $T(x)$ diagram is known for each section. However, the results for the $Cd_{2x}(AgIn)_{1-x}Te_2$ alloys already investigated [11], indicate that an annealing temperature of 600 °C should be satisfactory and this value was used here. Guinier X-ray powder photographs were used to check the equilibrium conditions of each sample and to determine whether a single-phase form was obtained. It was found that at least 30 to 40 days of annealing are necessary to obtain equilibrium conditions at 600 °C, since long-range diffusion may be required after the initial cooling from the melt. However, once this equilibrium has been achieved, the zincblende to chalcopyrite transition, which occurs below 700 °C and which involves only short-range diffusion, can occur in much shorter times, and samples showing room temperature equilibrium can be obtained by allowing the sample to cool in the furnace after switching off. Lattice parameter values were determined from the room temperature Gu inier photographs, with germanium used as an internal standard.

The DTA measurements [12] were made over a temperature range from 20 to 1050 °C using small quartz tubes provided with the usual re-entrant thermocouple position. The charge was approximately 100 mg for each sample and silver and gold were used as the reference materials. Both heating and cooling runs were carried out on each sample investigated.

Samples were prepared for optical absorption measurements by the usual method [13], slices of the ingots being polished down to give thin disc samples. The optical density $\ln(I_0/I_t)$ was measured as a function of photon energy $h\nu$ using a Cary 17 spectrophotometer. The values of $\ln(I_0/I_t)$ were corrected by subtracting a background value so as to give values proportional to the absorption coefficient α. The relation $(\alpha h\nu)^2 = C(E_0 - h\nu)$ was then used to obtain a value for the optical energy gap E_0.

3. DTA and X-Ray Results and Analysis

Samples were prepared to cover the complete composition range in steps of approximately 0.1 in x. DTA measurements were made on all of the samples and values of the various transition temperatures for each sample were determined. The resulting $T(x)$ diagram is shown in Fig. 1, where boundaries from the DTA data only are shown as full lines. The range of the present experimental set-up is from room temperature to 1150 °C. Thus since the melting point of ZnTe is approximately 1290 °C [2], it was not possible to obtain useful DTA data for samples with $x \geqq 0.55$, and so only estimates of the positions of the liquidus and solidus curves are shown as dashed lines in Fig. 1. The Guinier X-ray photographs showed that two single solid phase fields, viz. the chalcopyrite α-phase corresponding to $AgInTe_2$, the zincblende β-phase corresponding to ZnTe, plus a two solid phase $(\alpha + \beta)$ field occur in the composition diagram. Close to $x = 0$, i.e. in the chalcopyrite field, the structure was identified by the line splitting which occurs because $c/a \neq 2$. Appropriate lattice parameter values were determined for all samples, and the variation of the parameter a with the composition x is shown in Fig. 2. It is seen that, within the limits of experimental error, the variation of a with x can be taken as linear in both single-phase fields. In the two-phase $(\alpha + \beta)$ range, it is probable that the lattice parameter values vary with x, since, as indicated below, the tie-line does not lie in the plane of the diagram. In order to esti-

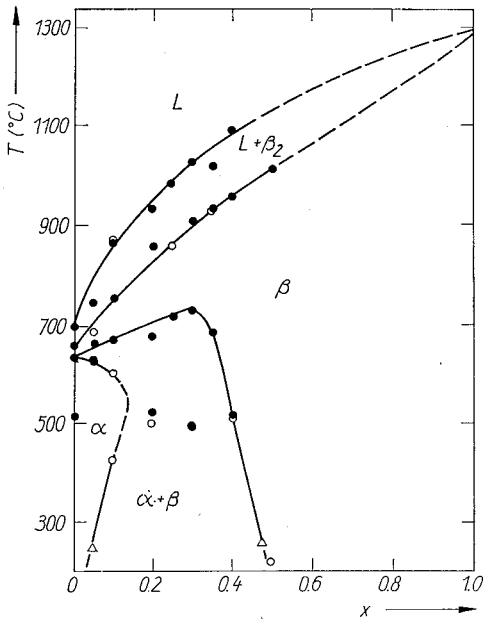

Fig. 1. $T(x)$ diagram for the $Zn_{2x}(AgIn)_{1-x}Te_2$ alloys. α is chalcopyrite and β zincblende structure. ○ DTA heating run, ● DTA cooling run, △ from X-ray data

mate the limits of single-phase behaviour, straight lines have been drawn through these values and the phase boundaries taken as the points of intersection of the appropriate lines of a versus x. Previous experience has indicated that in these types of materials, the conditions of slowly cooled samples represent the equilibrium conditions applicable for the temperatures 200 to 300 °C. Thus the above estimates have been taken as the boundaries of the α, (α + β), and β fields in this temperature range.

It is seen from Fig. 1 that the α-phase appears for $x = 0$ at $T \leqq 635$ °C and that the β-phase extends up to 660 °C, above which temperature it splits up into the two phases (L + β_2) which occur up to the liquidus point. These results are in reasonable agreement with those obtained by Chiang et al. [14] in the Ag_2Te–In_2Te_3 diagram, giving the α–β transition temperature as 649 °C. Palatnik and Rogacheva [15] gave a phase diagram for the Ag_2Te–In_2Te_3 system which shows the α–β transition of

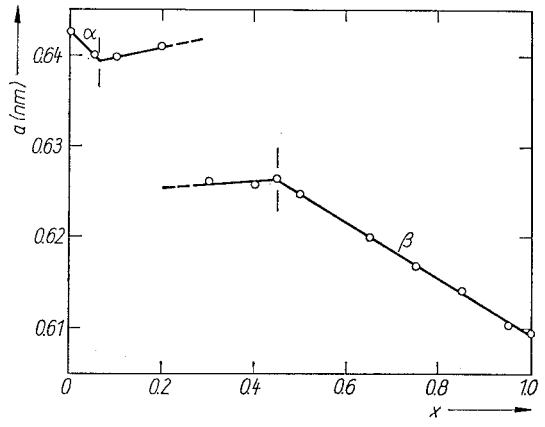

Fig. 2. Variation of lattice parameter a with x for the $Zn_{2x}(AgIn)_{1-x}Te_2$ alloys. α is chalcopyrite and β zincblende structure

$AgInTe_2$ at 537 °C. However, work by the present authors [11, 16, 17] on other diagrams involving $AgInTe_2$ shows better agreement with the results of Chiang et al. than with those of Palatnik and Rogacheva. The β- and β_2-phases are both zincblende but of different compositions.

With regard to the alloys, it is seen from Fig. 1 that the α-phase appears at 635 °C for $x = 0$ and that the field achieves a maximum width of ≈ 0.14 at 550 °C, below which temperature the range of solid solution is reduced as T is reduced. In the higher temperature range, the β-phase occurs at all compositions, and for $x \geqq 0.5$ it occurs at all temperatures below the solidus curve. The α- and β-fields are separated by a relatively wide two-phase (α + β) field. The shape of the boundary between the β and (α + β) fields indicates that the tie-lines of the (α + β) field cannot lie in the plane of the diagram, i.e. the section is not pseudobinary. As indicated above, this is consistent with the lattice parameter data and also with the optical energy gap results described below.

Above these solid phase fields, there is a two-phase (liquid + solid) field which terminates on the (L + α_2) region of the $AgInTe_2$ line, and the field has been labelled (L + α_2) to be consistent with this. The data for $AgInTe_2$ in the Ag_2Te–In_2Te_3 diagram [14] indicate that the α_2-phase is not represented by any point in the present section, so that the tie-lines of the (L + α_2) field again do not lie in the plane of the present diagram.

Finally, it is to be noted from Fig. 1 that peaks are observed in the range $0 \leqq x \leqq 0.4$ at temperatures of 500 to 520 °C. Similar results were found previously [11] for the $Cd_{2x}(AgIn)_{1-x}Te_2$ section. This apparent solid–solid transition may be correlated with photomicrograph data on $AgInTe_2$ [8], showing the appearance of small amounts of a second phase at the grain boundaries of samples annealed at 400 °C. This second phase may be associated with segregation of tellurium from the $AgInTe_2$ phase.

4. Optical Results

Optical absorption measurements were made at room temperature for all alloy samples. The resulting values of E_0 are shown in Fig. 3. Considering firstly the values in the single-phase β-field, i.e. $0.4 \leqq x \leqq 1.0$, it is seen that initially E_0 drops rapidly as the ternary compound is added to ZnTe, but that the curve flattens as x is reduced. This type of behaviour has been observed previously in a wide range of similar alloy

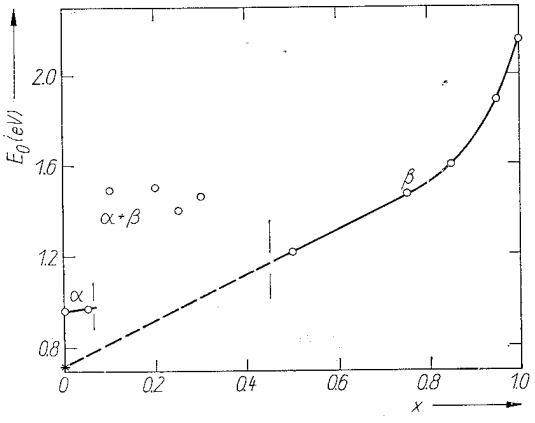

Fig. 3. Variation of room temperature energy gap E_0 with x for the $Zn_{2x}(AgIn)_{1-x}Te_2$ alloys. α is chalcopyrite and β zincblende structure

systems [6, 8, 18 to 20]. In previous work [16, 20], extrapolation from the cubic phase indicated that $AgInTe_2$ in the zincblende structure would have an optical energy gap of ≈ 0.7 eV. As indicated by the dashed line in Fig. 3, the present data are consistent with this value. In the chalcopyrite field, the limited range of solid solubility means that little data on the variation of E_0 with x can be obtained. However, the rate of variation of E_0 with x appears to be appreciably smaller than in the cubic case, the values of E_0 showing little change.

In Fig. 3, experimental values of E_0 determined for two-phase samples are shown, and it is seen that these are very different from the adjacent single phase values. This again is an indication that the tie-lines in this two-phase field do not lie in the plane of the diagram, so that the E_0-values do not correspond to any composition in the present section.

For alloys with a given structure, e.g. zincblende, and energy gap of the values obtained here, the variation of E_0 with composition is usually almost linear [21]. For the present alloys in the range of the zincblende structure, this type of behaviour is observed for $0.4 \leqq x \leqq 0.8$. However, for $0.8 \leqq x \leqq 1.0$, as indicated above, the value of E_0 changes rapidly and non-linearly with x. One factor which may cause this behaviour is the effect of p–d hybridization [22] between the Te p-states which form the valence band and the Ag d-states [4, 23]. This interaction causes the valence band to have some degree of d-character which increases as the Ag content is increased, i.e. as x is decreased, and which causes a reduction in the value of E_0 [23]. From the variation of E_0 in Fig. 3, this interaction appears to cause maximum reduction in E_0 with the initial addition of Ag to the II–VI compound.

In the case of alloys with chalcopyrite structure, the variation of E_0 with x is less than for the zincblende range $0.4 \leqq x \leqq 0.8$. In this case, further factors which affect the E_0-variation are the standard structural effects observed in chalcopyrite materials, such as tetragonal distortion and cation displacement [22].

5. Conclusions

For the $Zn_{2x}(AgIn)_{1-x}Te_2$ section, the X-ray experimental results show that below the solidus curve there are two single-phase fields, viz. the calcopyrite α and the zincblende β fields, plus a two-phase ($\alpha + \beta$) field. The variation of the lattice parameter a with x is linear for each single-phase field, and the slope discontinuities of the a versus x graph give a good indication of the boundaries of the single-phase fields. The various results indicate that in the two-phase ($\alpha + \beta$) field, the tie-line does not lie in the plane of the section. Over the whole composition range, the β-field is bounded by a two-phase ($L + \beta_2$) field, and the tie-lines of this field also do not lie in the plane of the section. Thus the section does not show pseudobinary behaviour.

For samples with $0 \leqq x \leqq 0.4$, the DTA data showed peaks at temperatures of 500 to 530 °C which are due to segregation of another phase. This additional phase may be associated with segregation of tellurium from the main phase.

The form of the E_0 versus x curve is typical of alloys of this type [6, 8, 18 to 20] and extrapolation from the zincblende range shows that $AgInTe_2$ in the zincblende structure would have an E_0 of ≈ 0.7 eV in good agreement with previous work [16, 20].

Acknowledgements

The authors wish to thank G. S. Pérez and F. Sanchez for assistance in the experimental measurements, and members of the Crystallography Section of the Chemistry Department of the University of the Andes for the facilities of the X-ray laboratory.

Original Papers

phys. stat. sol. (a) **111**, 405 (1989)

Subject classification: 61.60; 64.75; S8.16

Laboratorio de Cristales, Centro de Estudio de Semiconductores, Departamento de Física, Facultad de Ciencias, Universidad de Los Andes, Mérida[1])

Phase Diagram, Lattice Parameter, and Optical Energy Gap Values for the $Zn_{2x}(AgIn)_{1-x}Te_2$ Alloys

By

R. Tovar, M. Quintero, P. Grima, and J. C. Woolley[2])

Polycrystalline samples of $Zn_{2x}(AgIn)_{1-x}Te_2$ alloys are prepared by the melt and anneal technique. Differential thermal analysis measurements are carried out on the alloys and the $T(x)$ diagram is determined. Guinier X-ray powder photographs are used to show the equilibrium conditions and to give lattice parameter values. Two single solid phase fields are observed in the diagram, which is shown not to be pseudobinary. Room temperature optical energy gap values are determined as a function of composition.

Aus der Schmelze und mittels Temperungstechnik werden polykristalline Proben von $Zn_{2x}(AgIn)_{1-x}Te_2$-Legierungen hergestellt. Differentielle Thermoanalyse wird an den Legierungen durchgeführt und das $T(x)$-Diagramm bestimmt. Guinier-Röntgen-Pulverphotogramme werden benutzt, um die Gleichgewichtsbedingungen zu zeigen und um die Werte des Gitterparameters anzugeben. Zwei Einzel-Festphasenfelder werden im Diagramm beobachtet, das sich als nicht pseudobinär erweist. Die Werte der optischen Energielücke bei Zimmertemperatur werden als Funktion der Zusammensetzung bestimmt.

1. Introduction

There is considerable interest in the II–VI and I–III–VI_2 compounds and their alloys, because of their potential use in technological applications such as solar-energy conversion, infra-red radiation detectors, etc. [1]. Alloys of pairs of II–VI compounds have been investigated in some detail [2, 3], also mixed alloys of I–III–VI_2 compounds have received attention [4, 5]. Work on the pseudobinary I–III–VI_2–2(II–VI) alloys has been carried out for a number of systems, e.g. $Cd_{2x}(CuIn)_{1-x}Te_2$ [6, 7], $Cd_{2x}(AgIn)_{1-x}Te_2$ [8], $Zn_{2x}(CuIn)_{1-x}Te_2$ [9], and $Zn_{2x}(CuGa)_{1-x}Te_2$ [10], but little work has been done on alloys combining Ag and Zn.

The $AgInTe_2$ compound and its alloys are of interest as materials for near-infrared-light detectors and improvements in performance and a shift towards the visible range may be obtained with the addition of ZnTe. For this application, knowledge of the range of solid solubility, crystallography, and optical energy gap values of the system $Zn_{2x}(AgIn)_{1-x}Te_2$ is required. In the present work, differential thermal analysis (DTA) measurements have been made to give the $T(x)$ diagram of the system, and values have been determined for lattice parameter and optical energy gap.

---

[1]) Mérida, Venezuela.

[2]) Permanent address: Physics Department, University of Ottawa, Ottawa, Ontario, Canada K1N 6N5.